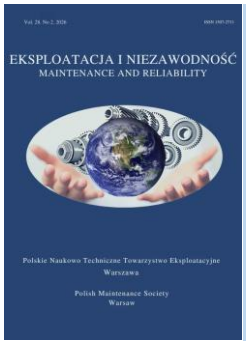

Eksploatacja i Niezawodnosc – Maintenance and Reliability
Volume 28 (2026), Issue 2
journal homepage: http://www.ein.org.pl

Article citation info:
Zhu G, Liu X, Huang Q, A Time-Weighted Fusion Waveform Factor Based Health Indicator for Condition Monitoring of Rotating Machinery, Eksploatacja i Niezawodnosc – Maintenance and Reliability 2026: 28(2) http:/10.17531/ein/214295

A Time-Weighted Fusion Waveform Factor Based Health Indicator for Condition Monitoring of Rotating Machinery

Indexed by: Web of Science Group

Guanhua Zhu[a], Xuebin Liu[a,*], Quansi Huang[a]

[a] Guangdong Provincial Key Laboratory of Petrochemical Equipment and Fault Diagnosis, Guangdong University of Petrochemical Technology, Maoming 525000, China, China

Highlights

- A new health indicator is proposed for monitoring rotating machinery.
- An optimization algorithm is used to tune key parameters and analyze sensitivity.
- Tested on a public bearing dataset to detect faults earlier than other methods.
- Further tested on industrial equipment data to demonstrate the method's effectiveness.

Abstract

In rotating machinery condition monitoring, traditional health indicators (HI), including quantitative and dimensionless forms, are widely used for health assessment. However, such indicators often respond slowly to early faults or display decreasing and oscillatory trends after fault onset, causing delayed monitoring and economic losses. To address these issues, this study proposes a novel HI termed the time-weighted fusion waveform factor (T2WF). Derived from the conventional waveform factor (WF), T2WF introduces the concept of periods, computes dimensionless values in proximal and distal periods, and combines them through a weighting parameter. The Northern Goshawk Optimization Algorithm (NGOA) is employed to optimize the key parameters. Validation is conducted on the public XJTU-SY dataset and on rotating machinery datasets from two petrochemical enterprises. Experimental results show that T2WF achieves earlier fault detection and superior diagnostic performance compared with traditional HI, international standards, and deep learning methods.

Keywords
condition monitoring of rotating machinery, time-weighted fusion waveform factor, health indicator, optimization algorithm

1. Introduction

Rotating Machinery is an indispensable core equipment in modern industrial systems, which is widely used in electric power, petrochemical, aerospace, metallurgy, transportation and other fields. Rotating machinery is mainly composed of rotor and stator [1], and the rotor realizes the conversion or transfer of energy through rotation. The operational performance of rotating machinery directly affects the production efficiency and safety, so the monitoring of its health status and fault diagnosis is of great significance [2]. Health indicator (HI) is an important and effective tool to realize the condition monitoring of machinery and equipment, which is still the mainstream of industrial field monitoring [3,4].

HI can be divided into two categories: quantitative indicators and dimensionless indicators. The quantitative indicators retain the physical units of the signal, such as the root mean square (RMS), peak, and so on. This type of indicators is more sensitive to the fluctuation of working conditions, and has better stability and intuition under constant working conditions [5]. RMS is one of the most commonly used quantitative HI in the field of mechanical signal processing and fault monitoring.

(*) Corresponding author.
E-mail addresses: G. Zhu (ORCID: 0009-0009-4247-6713) zhugh@gdupt.edu.cn, X. Liu (ORCID: 0009-0002-1635-2230) 1055751538@qq.com, Q. Huang (ORCID: 0009-0003-6501-3099) huangquansi1999@gmail.com

It is also used as a key indicator in international standards [6], which reacts to the physical significance of the energy contained in the machinery to monitor the degree of damage to rotating machinery, however, the real-time nature of its alarms is delayed because of its strong dependence on the experience of experts [7]. Dimensionless HI are obtained by normalizing the original vibration signals, which do not carry physical units, and can maintain strong fault identification ability under different loads, speeds and other complex working conditions. Including kurtosis, waveform factor(WF), pulse factor and margin factor, etc., these indicators emphasize the changing characteristics of the signal pattern, especially in the characterization of shock-type faults and non-Gaussian characteristics, and have been widely used in early fault monitoring and health assessment of rolling bearings, gearboxes and other rotating machinery [8-10]. Indicators such as margin factor and impulse factor are highly sensitive to shock signals [11,12], but they are also sensitive to noise or episodic shocks and are easily disturbed. In response to the dilemmas arising from the above, some new methods are emerging. Ni et al [13] constructed a new HI by combining spectral correlation and Wasserstein distance and linear rectification, which is able to reveal the weak degradation information of rotating machinery buried by noise. Song et al [14] constructed the HI by combining the principal component cumulative empirical distribution model) to solve the problem of the problems of high cost of data collection and limitation of usage conditions in the construction of traditional HI. Wang et al [15] constructed sparse metrics from kurtosis and noise energy for machine health monitoring. Song et al [16] proposed a constructed synthetic shock index, which utilizes the product of autocorrelation coefficients to differentiate between the effective shock component and the noise.Hu et al [17] proposed a multiscale dimensionless metric. After multi-resolution decomposition of vibration signals, the dimensionless index is calculated at each scale to obtain multi-scale features to improve the accuracy of rotating machinery condition monitoring identification. Gao et al [18] proposed a sliding window linear regression method for every 50 RMS values as a group, fit a straight line to the RMS values within the group to obtain the RMS growth rate, and use the rate threshold to determine the starting point of bearing aging.

In summary, HI are widely used in the field of rotating machinery, but there are still some limitations in terms of sensitivity and timeliness of fault identification [19,20]. On the one hand, dimensionless indicators are usually difficult to accurately and effectively monitor potential early weak fault information [21,22], and most of the traditional HI ignore the possible dynamic degradation characteristics of the signal in different time periods, and there are problems such as response lag in dealing with the early stage of fault development and untimely warning of faults, which leads to limited monitoring effect [23]. Therefore, there is an urgent need to design HI that have time sensitivity and can significantly advance the response time of fault alarms in order to improve the identification of early faults and meet the higher requirements of real-time and accuracy of monitoring in industrial sites. The main contributions of this paper include:

1. A novel HI, the time-weighted fusion waveform factor (T2WF), is proposed. It is sensitive to early faults and is constructed by the weighted fusion of dimensionless indicators of vibration signals collected during the proximal and distal periods.
2. The Northern Goshawk Optimization Algorithm (NGOA) is introduced to optimize the key parameters of T2WF, and a detailed parameter sensitivity analysis is conducted.
3. The proposed method was evaluated on the publicly available dataset, demonstrating earlier detection of fault fluctuations and more precise fault localization than international standards, traditional metrics, and current deep learning approaches, with spectral validation confirming its effectiveness.
4. Further validation of the proposed method was conducted using two equipment datasets from a Chinese petrochemical enterprise. The first dataset was collected from a gearbox with misalignment between the high-speed shaft and the compressor, and the second dataset was collected from a compressor rotor affected by impeller fouling, leading to dynamic imbalance fault characteristics. The experimental results from both datasets fully confirm the effectiveness of the proposed method.

2. The proposed method

In order to improve the accuracy and response speed of early failure identification of rotating machinery, it is especially

critical to construct HI with timeliness. In this section, we first summarize and analyze the existing commonly used HI, covering two types of methods, namely, quantitative and non-quantitative, and discuss their applicability and limitations under actual working conditions. Based on the problems that traditional indicators respond slowly to sudden failures and are susceptible to noise interference, this paper proposes a T2WF that integrates time-scale information. The indicator realizes sensitive monitoring of weak degradation signals by integrating short-term and long-term vibration characteristics. Meanwhile, in order to subsequently improve its parameter adaptability, this paper introduces the NGOA as a potential optimization tool to optimize and adjust the key parameters.

2.1. Commonly used HI

RMS is a basic measure of the energy distribution of a signal that reflects the overall amplitude level of the signal. With strong noise immunity, RMS is commonly used in rotating equipment such as bearings and gearboxes to assess the overall health of the system or the load level [24].

$$RMS = \sqrt{\frac{1}{N}\sum_{n=1}^{N}|x(n)|^2} \tag{1}$$

Where $x(n)$ is the time series data of N (n=1,2,...,N) data points.

The mean is the arithmetic average of the data points in the signal data, which reflects the central tendency of the signal. It is usually used to describe the average level of the signal and to analyze the overall trend of the data [25].

$$Mean = \frac{1}{N}\sum_{n=1}^{N} x(n) \tag{2}$$

Waveform Factor (WF), used to highlight short-lived spikes in a signal. It is sensitive to minor, short-lived shocks and can detect transient pulsed vibrations in the early stages of a fault [25].

$$WF = \frac{\sqrt{\frac{1}{N}\sum_{n=1}^{N}|x(n)|^2}}{\frac{1}{N}\sum_{n=1}^{N}|x(n)|} \tag{3}$$

Peak Factor (PF) describes the ratio between the extreme value and the RMS value of a signal and is often used to monitor the presence of spike-like outliers in the signal, with larger values indicating a higher likelihood of a sudden shock [25].

$$PF = \frac{max|x(n)|}{\sqrt{\frac{1}{N}\sum_{n=1}^{N}|x(n)|^2}} \tag{4}$$

Spectral Kurtosis (SK) is a measure of the kurtosis of a signal in the frequency domain, which can assess the presence of transient shocks or noise interference in the signal. Its calculation reveals how sharp or smooth the signal is in the frequency domain [26].

$$SK = \frac{\sum_{n=1}^{N} F[x(n)]^4}{\left(\sum_{n=1}^{N} F[x(n)]^2\right)^2} \tag{5}$$

Where $F[x(n)]$ is the Fourier transform of the signal $x(n)$ in the frequency domain and represents the individual frequency components of the signal in the frequency domain.

2.2. Proposed HI

The WF, as a dimensionless HI, can effectively reflect the instantaneous impulse changes in the signal by measuring the waveform characteristics of the signal and shows high sensitivity to short-time shock signals [25].

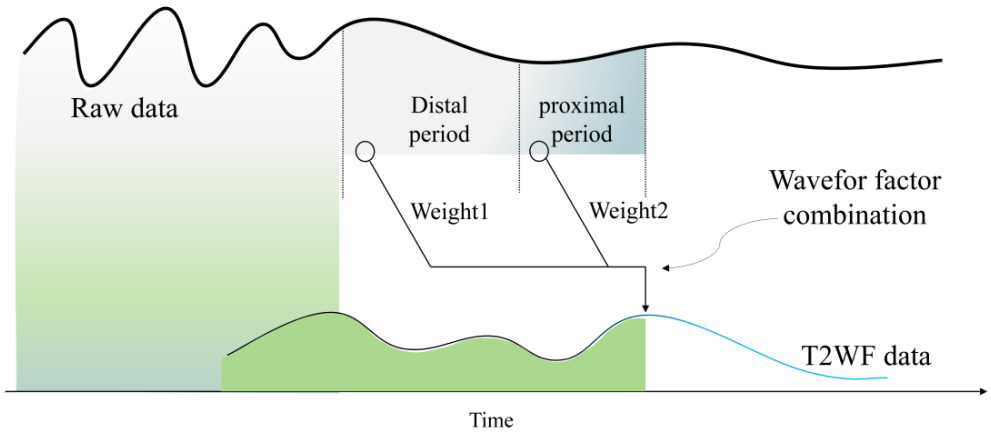

Figure 1. Time-weighted fusion waveform factor.

However, the traditional WF may have certain limitations in practical applications, especially in complex environments

where signal interference or noise exists, which is manifested in the lack of fault identification ability and response speed [27]. In order to overcome this problem, T2WF proposed in this paper introduces a time-weighted fusion design based on the traditional WF, i.e., it combines the WF computed within the proximal and distal periods. The advantage of this approach is that it is able to focus on both short-term sudden shock changes and long-term stability changes, which improves the sensitivity to detect faults, especially in the early stage of equipment faults, which can be recognized and warned at an early stage.

As shown in Figure 1, the design of the T2WF indicator realizes the weighted fusion of the WF calculated in the proximal period and those calculated in the distal period through the weight adjustment mechanism. Specifically, the proximal period WF focuses on responding to sudden changes in the current signal, while the distal period WF focuses on the long-term stability of the signal. On this basis, the degree of influence of both on the final HI can be dynamically adjusted by the introduction of the weighting factor, so that the indicator can adaptively change according to the actual working conditions. For the proximal period, we enhance its response to short-term failures by adjusting the length of the window; for the distal period, the long-term stability and trend of the equipment is captured by adjusting the size of the window. Specifically, the mathematical expression of the T2WF indicator is as follows:

$$F_p(k) = \frac{\sqrt{\frac{1}{L}\sum_{i=k-T_p}^{k-1}|x(i)|^2}}{\frac{1}{L}\sum_{i=k-T_p}^{k-1}|x(i)|} \tag{6}$$

$$F_d(k) = \frac{\sqrt{\frac{1}{L}\sum_{i=k-T_d}^{k-T_{p-1}}|x(i)|^2}}{\frac{1}{L}\sum_{i=k-T_d}^{k-T_{p-1}}|x(i)|} \tag{7}$$

Where T_p is the proximal period, T_d is the distal period, $x(i)$ is the original sample data collected at i, L is the sample length, k represents the number of samples, $F_p(k)$ is the distal period WF, and $F_d(k)$ is the distal period WF.

The T2WF introduces the proximal period to focus on the current mutation, and combines with the distal period to reveal the signal stability of the longer period, and introduces the discrete values of weights, which control the degree of fusion of the dimensionless features of these two periods. With this weighting strategy, T2WF is able to adaptively adjust the degree of focus on different time-period features so as to respond in real time according to the characteristics of the signal, as follows.

$$\Phi(k) = \frac{MF_p(k)+F_d(k)}{M+1} \tag{8}$$

Where $\Phi(k)$ is the T2WF HI and M is the weight.

In this design, the proximal period is used to strengthen the sensitivity to sudden vibration changes at the current time point, while the distal period is used to provide a global trend reference to suppress local noise perturbations. The weight M realizes the adaptive response capability to the features under different operating conditions by adjusting the relative influence of the two. Further, this paper proposes the following constraint strategies for the above key parameters to guarantee the real-time and robustness: the initial monitoring moment is taken by the distal period, and the value of the distal period T_d should satisfy the value of T_d>T_p, and be controlled within 50 to ensure the rapid response of the indicator to early anomalies, which is used to enhance the long-term trend capture capability, The range of M is limited to 50, and is used as an optimization parameter to search for the optimal value in the algorithm.

2.3. The Northern Goshawk Optimization Algorithm

The Northern Goshawk Optimization Algorithm (NGOA) [28] simulates the hunting behavior of a goshawk through a two-stage strategy: long-distance approach for global exploration and short-range pursuit for local exploitation, achieving a balance between the two. Unlike traditional algorithms, NGOA updates position matrices directly without relying on velocity vectors, and requires only two core hyperparameters: population size and maximum iterations. Its computational complexity is comparable to Genetic Algorithms (GA) and Particle Swarm Optimization (PSO).GA performs search through selection, crossover, and mutation, while PSO relies on individual and global best positions with inertia weight to update velocity. In contrast, NGOA eliminates the need for chromosome encoding and parameter tuning, offering a simpler structure, smoother convergence, and reduced risk of premature convergence.

Experimental results show that NGOA achieves faster convergence and better solution quality, especially in high-dimensional and multi-modal optimization problems [28]. It also demonstrates stronger robustness with fewer parameter dependencies.

The algorithm achieves efficient search and global exploration of the optimal solution by abstractly simulating a series of dynamic behaviors as described above. In the 1st hunting phase of the Northern Goshawk, it will randomly select a prey and then quickly launch an attack. In this stage, the mathematical expression of the behavior of the NGOA is specifically formulated as follows:

$$u_{i,j}^{new,p1} = \begin{cases} u_{i,j} + r\left(p_{i,j} - Eu_{i,j}\right) & F_{p_i} < F_i \\ u_{i,j} + r\left(u_{i,j} - p_{i,j}\right) & F_{p_i} \geq F_i \end{cases} \tag{9}$$

Where F_{p_i} is the objective function value of the prey position of the *i*th northern goshawk, i.e., the adaptation value; F_i is the objective function value of the *i*th northern goshawk; $p_{i,j}$ represents the position of the prey selected by the *i*th goshawk in the *j*th dimension; $u_{i,j}^{new,p1}$ is the new state of the *i*th northern goshawk in the *j*th dimension in the 1st hunting stage; $u_{i,j}$ is the state of the *i*th northern goshawk in the *j*th position; r is the random number belonging to [0,1], and E takes the value of 1 or 2.

In the 2nd hunting phase, after the northern goshawk attacks the prey, the prey will try to escape. Assuming that this prey is in the attack position at the radius R_h, the mathematical expression for the 2nd hunting stage is given as follows:

$$\begin{cases} R_h = 0.02\left(1 - \frac{A}{\tau}\right) \\ u_{i,j}^{new,p2} = u_{i,j} + R_h(2r-1)u_{i,j} \end{cases} \tag{10}$$

Where A is the current number of iterations; τ is the maximum number of iterations; $u_{i,j}^{new,p2}$ is the new state of the *i*th northern goshawk in the *j*th dimension in the 2nd hunting stage.

In the 2nd hunting stage of NGOA, the Levy flight strategy is introduced to update the position of the northern goshawk to avoid the population falling into the local optimum and to expand the search capability, the specific formula is as follows:

$$L_{Levy}(\beta) = \frac{\mu}{|v|^{\frac{1}{\beta}}} \tag{11}$$

Where $L_{Levy}(\beta)$ is the step size of Levy flight; $\beta = 1.5$; μ, v obey normal distribution, and the specific equations of σ_μ and σ_v are as follows:

$$\begin{cases} \sigma_\mu = \left\{ \frac{\Gamma(1+\beta)\sin(\frac{\beta\pi}{2})}{\Gamma(\frac{1+\beta}{2})\beta 2^{\frac{\beta-1}{2}}} \right\}^{\frac{1}{\beta}} \\ \sigma_v = 1 \end{cases} \tag{12}$$

where Γ denotes the Gamma function.

3. Sensitivity analysis and optimization experiment of T2WF parameters

We constructed the T2WF, a novel HI, and elaborated its basic principle of fusing features of different time scales to enhance fault identification. However, the indicator contains several key parameters in practical application, such as proximal period, distal period and weight. The setting of these parameters directly affects its monitoring sensitivity and warning effect. Therefore, in order to optimize the performance of the indicator, this section will carry out a parameter sensitivity analysis around T2WF to systematically evaluate the impact of each parameter on the timeliness of fault warning. At the same time, the NGOA is used to intelligently search for optimal parameter combinations to ensure that the indexes have excellent performance under a variety of working conditions, providing a reliable parameter basis for subsequent experimental validation.

3.1. Parameters sensitivity analysis

In order to conduct sensitivity analysis of T2WF, it is first necessary to define the input data and output results. In section 3, we choose the Bearing1_2 dataset from the XJTU-SY dataset to conduct the sensitivity analysis of T2WF. This paper focuses on the application of rotating machinery HI in reliability management, especially the criticality of early failure detection. T2WF is able to clearly demonstrate the process of failure evolution, and this feature is of great significance in practical applications. With respect to the three key parameters involved in the new indicator, this paper carries out a correlation analysis of the effect of parameter adjustment on the advancement of warning, and observes the effect on the advancement time of failure warning by adjusting these parameters. Since these parameters directly affect the sensitivity of monitoring, the analysis of the impact of parameter regulation on warning advancement allows us to clarify the extent of the impact of each parameter on the performance of the indicator and to assess its contribution to the fault warning lead time. Firstly, the values of the proximal and distal period are fixed, and by adjusting the weights, the impact of setting different weights on the fault warning lead time and sensitivity is analyzed. In this way, we can explore the specific impact of individual parameter changes on the performance of the early warning model, i.e., we will

subsequently fix the other parameters separately, adjust the parameter values one by one, and assess their impact on the performance of the system. In order to reflect the superiority of the research results of this paper, the initial parameters of this experiment are set as follows: $T_p = 2$, $T_d = 9$, and $M = 8$, and the results of analyzing the experiments are shown in Figure 2, and the data of sensitivity analysis of M are shown in Table 1, and the data of sensitivity analysis of proximal period parameters are shown in Table 2, the sensitivity analysis data of distal period parameters are shown in Table 3.

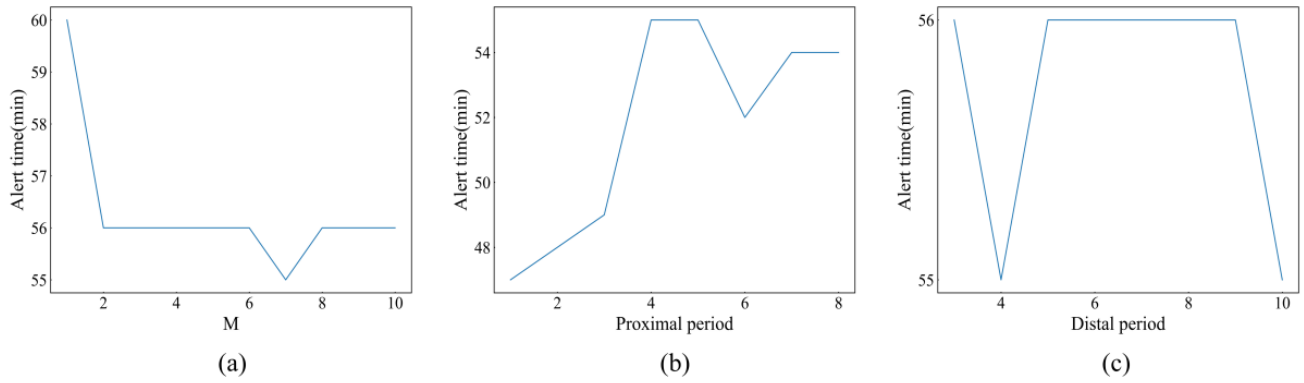

Figure 2. Sensitivity analysis of monitoring indicators.

In summary, the following conclusions can be drawn.

Changes in M show a sharp downward trend on the alarm time. there is a gradual downward trend in the alarm time when the value of M ranges from 1-2. The alarm time remains stable in the interval when the value of M increases from 2 to 5. This pattern suggests that changes in M within a certain range have a smoother effect on the alarm time, whereas when M reaches 7, the alarm time starts to advance. This result may imply that the system is more sensitive to proximal information when M exceeds a particular value, thus advancing the alarm time. This advancement, although relatively small, may have some practical significance for real-world applications, especially in systems that rotate at high speeds.

The change of the proximal period causes the fluctuation of the alarm time to show a trend of rapid rise, reaching a peak, and then remaining stable. The overall trend is that the alarm time rises as the proximal period increases. When the proximal period is between 1 and 4, the alarm time increases from 47 minutes to 55 minutes, which is a more obvious change, which may indicate that there is a positive correlation between the increase of the proximal period and the alarm time in this interval. Beyond 5, the alarm time continues to fluctuate but is relatively smooth compared to before, and also begins to show a tendency for the alarm time to advance, suggesting that the effect of the proximal period on the alarm time plateaus at this stage and the changes become less sensitive.

The overall trend of the distal period shows that the alarm time oscillates and fluctuates between 55 and 56 minutes, with very small changes. When the distal period is 4, the alert time drops slightly to 55 minutes, then stays at 56 minutes between 5 and 9, and finally drops slightly back to 55 minutes at 10. Overall, the alarm time fluctuates within the range of 55 to 56 minutes with very slight variations and can almost be considered stable. This suggests that changes in the distal period have a small effect on the alert time, and that fluctuations in the distal period within that range do not cause significant alert time changes. Therefore, the distal period has a more limited moderating effect on alert times, and the overall trend shows a more stable state.

Table 1. sensitivity analysis of weight.

M	T_p	T_d	Alert time(min)
1	2	9	60
3			56
5			56
7			55
9			56

Table 2. Sensitivity analysis of proximal period.

M	T_p	T_d	Alert time(min)
5	2	9	48
	4		55
	6		52
	8		54

Table 3. Sensitivity analysis of distal period.

M	T_p	T_d	Alert time(min)
5	2	4	55
		6	56
		8	56
		10	55

3.2. Parameters Optimization of T2WF HI

The performance of T2WF is closely related to the selection of parameter scales, but the parameter tuning process is cumbersome, in order to simplify this process, this paper introduces the NGOA, the detailed process can be seen in Figure 3, through which the algorithm regulates the three key parameters of T2WF. In this process, a fitness function needs to be defined as the optimization objective of the optimization algorithm. To ensure that the fitness function matches the actual fault diagnosis task, we take the example of using the Bearing1_2 dataset and adopt the 3σ criterion [29] as the alarm threshold. Specifically, the fitness function aims to take into account both the timing of alarms and the alarm amplitude. We set the alarm threshold as the mean plus three times the standard deviation of the data, and the early or late alarm moment is crucial for fault detection, so we use the time of the first alarm as the numerator of the fitness function, while the amplitude corresponding to the alarm moment is used as the denominator. The purpose of this design is to make the fitness function as early as possible under the condition of large alarm amplitude through the optimization of NGOA, so as to improve the ability of early fault detection, and the specific fitness function is set as the following equation:

$$F_{fitness} = min\left(\frac{t_\alpha}{Y_\omega}\right) \tag{13}$$

Where t_α is the first alarm time, Y_ω is the corresponding monitoring index value at the first alarm. $F_{fitness}$ is fitness function.

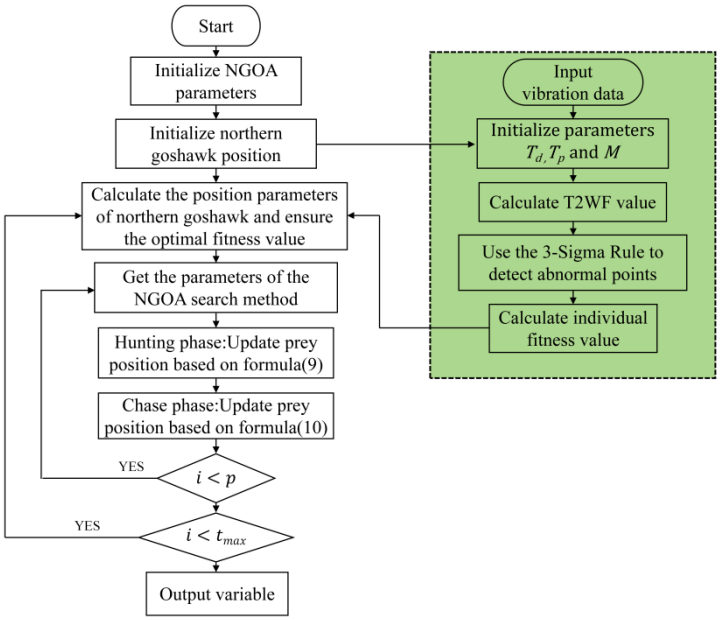

Figure 3. Parameter optimization flowchart.

In this experiment, the initial parameters of the optimization algorithm are set randomly, the fitness function is defined according to Equation (13), and the parameter optimization is adopted by NGOA. the population size is set to 50, and the maximum number of iterations is 100. Figure 4(a) demonstrates the convergence curve of fitness on the training dataset. Thanks to the excellent global search capability of NGOA, the optimization process effectively avoids the risk of falling into local optimum. When iterating to the 4-th generation, the algorithm rapidly converges and obtains the optimal fitness value, showing excellent convergence speed. The finalized optimal parameters are: T_p = 2.35, T_d = 3.02, and M = 1.23. Figure 4(b) shows the result plots of the exhaustive enumeration method, which aims at verifying the convergence of the NGOA. To realize the exhaustive enumeration, we have rounded all the parameters so that the exhaustive enumeration method can be executed at an acceptable computational complexity. In this setting, the optimal parameter combinations obtained by the

exhaustive enumeration method are: $T_p = 2$, $T_d = 3$, and $M = 1$, which are highly consistent with the results obtained by the NGOA, thus verifying the convergence reliability of the NGOA in this task.

The final obtained parameter values will be applied in the setting of the T2WF parameters in the Bearing2_2 dataset discussed in Section 4. In addition, all the petrochemical plant type 2 rotating machinery datasets presented in Section 4 are analyzed using the T2WF-NGOA method, and their optimization parameters are detailed in Table 4.

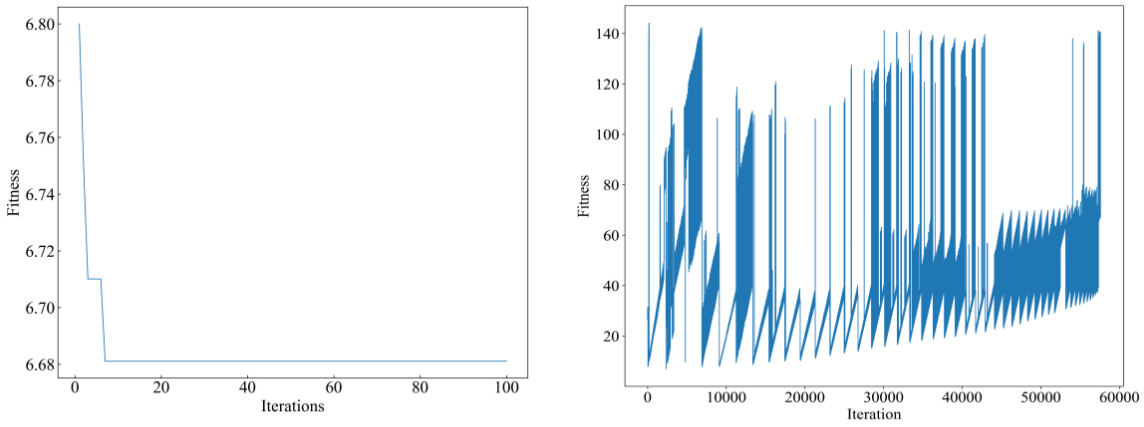

(a) (b)

Figure 4. Comparison between NGOA and the exhaustive enumeration method.

Table 4. Parameters Obtained by NGOA from the Petrochemical Dataset.

Number.	Dataset name	T_p	T_d	M
a	Main fan unit	10.43	21.02	1.56
b	Compressor	2.41	3.38	4.10

4. Experimental validation and discussion

After completing the sensitivity analysis and optimization of the key parameters of the T2WF HI, this chapter will focus on the systematic experimental validation of its practicality and generalization capability. The performance of T2WF under different operating and equipment conditions is evaluated through comparative analyses on several typical datasets covering the failure evolution process, including the publicly available XJTU-SY rolling bearing life data and actual working condition data from two petrochemical companies. The experiment not only covers the comparison with traditional HI (e.g., RMS, SK, WF, etc.), but also incorporates the current more advanced deep learning methods as a reference to comprehensively examine the advantages of T2WF in early warning, trend monotonicity and anti-interference ability. Meanwhile, the physical reasonableness of the warning moments is verified through spectral analysis to ensure the correctness of the indicator response.

4.1. Dataset Description

4.1.1. XJTU-SY dataset

Xi'an Jiaotong University has collaborated with SY to conduct accelerated life tests on rolling bearings and has opened the related dataset to the global research community. The project provides an important data resource for academia and advances fault diagnosis and health monitoring technology in industry. The test platform includes an AC motor, motor speed controller, hydraulic loading system, etc. It is capable of performing accelerated life tests under different working conditions, mainly regulating radial force and speed. The bearing vibration signals are collected using PCB 352C33 acceleration sensor, and the data are recorded by DT9837 signal collector with a sampling frequency of 25.6 kHz, a sampling interval of 1 minute, and a sampling duration of 1.28 seconds each time. Each sampling data is stored as a csv file, named in chronological order.

4.1.2. Industrial petrochemical dataset

In this study, reactor vibration signal data from two typical petrochemical companies in China were collected by a wireless vibration sensor monitoring system. The dataset contains the vibration signals of the main fan unit of the catalytic cracking unit and the high-pressure cylinder equipment of the syngas unit

of the coking unit, and the unit of data is mm/s. The corresponding fault types of each dataset are detailed in Table 5. When the vibration amplitude of the equipment exceeds the preset warning threshold, the data acquisition system will automatically adjust the sampling interval. All vibration signals are saved to a specified folder, and the recorded txt file contains the current rotational speed, sampling frequency, time stamp and 1024 time-domain vibration data points. Figure 5 shows the equipment destruction from two datasets taken during overhaul, and Table 5 shows its details.

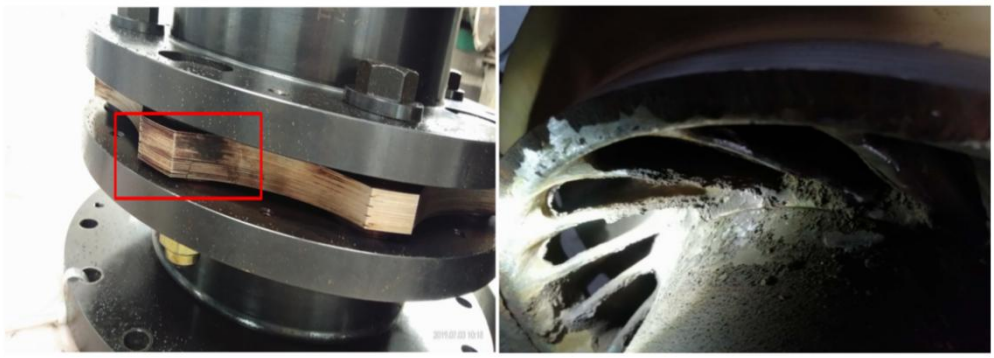

(a) (b)

Figure 5. Damage conditions in the petrochemical dataset.

Table 5. Detailed Information of the Petrochemical Enterprise Dataset.

Number	Dataset name	Damage location	Fault type	Rated speed
a	Main fan unit	Shaft system between high speed shaft and compressor	Misalignment	5900r/min
b	Compressor	Rotor	Dynamic unbalance due to fouling	10550r/min

4.2. Comparison experiment of HI on XJTU-SY dataset

In this study, we have chosen the XJTU-SY bearing dataset as the experimental data source with the aim of verifying the effectiveness of the proposed method in fault warning and its generalization ability. We apply the parameters obtained in Section 3.2 to the Bearing2_2 dataset for the experiments, aiming to evaluate the adaptability of the model on different individuals, while reflecting the generalization performance of the metric.

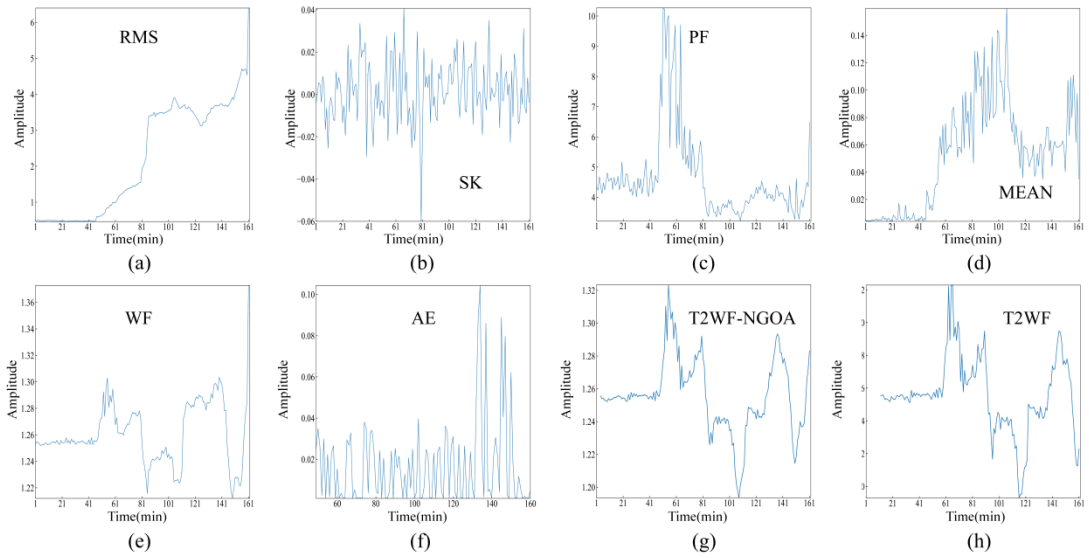

Figure 6. Monitoring curves for each indicator of bearing 2_2.

Table 6. First Alarm Time for Each Indicator in Bearing 2_2.

Indicator	Alert time(min)	Indicator	Alert time(min)
RMS	90	WF	139
SK	107	AE	133
PF	59	T2WF-NGOA	52
MEAN	67	T2WF	55

The numerical results of the experiments are presented in Table 6, and the image results are displayed in parts (a) to (h) of Figure 6, where (a) to (h) correspond to the commonly used health metrics such as RMS, SK, PF, and mean value, respectively. In addition, we introduce a deep learning method based on autoencoder (AE) [30,31], T2WF metrics optimized by NGOA, and T2WF metrics under random parameter conditions. We will compare them using the methods specified in the international standard [6], which mainly specifies the basic requirements and methods for measuring and evaluating vibration of mechanical equipment on non-rotating mechanical components. The standard sets warning threshold parameters for different power levels of RMS, so that the RMS warning threshold is set to 3.5 mm/s. The upper confidence interval, i.e., the mean plus three times the standard deviation, of the guideline of the warning indicator 3 σ commonly used in industry is also set as the warning threshold. When the monitored value exceeds this threshold, the system will trigger a fault warning. This method can not only effectively monitor potential faults, but also provide a reliable basis for early warning.

It should be especially pointed out that the comparison method of the AE structure is of great significance in this study. Deep learning methods are particularly suitable for data-driven fault monitoring [32]. In order to compare with the traditional methods, we used an AE-based approach to generate reconstruction errors. In this method, we designed an encoding stage that contains a linear layer and a bidirectional long-short-term memory (Bi-LSTM) network, and a decoding stage that is constituted by a linear layer. In our experiments, we used 30% of the data for training, set 500 epochs with Adam optimizer and learning rate set to 0.001, and the rest of the data was used for testing, generating reconstructed data and calculating the reconstruction error.

The results show that only the PF and WF showed large fluctuations in the early part of the data in the traditional health metrics. The reconstruction error of the AE method was maintained at a low level until 130 minutes, but suddenly spiked at 133 minutes, suggesting that the data in this segment was not smooth, which in turn issued a fault warning. In contrast, the RMS and mean value metrics showed a slow upward trend and did not generate an early warning in the early period. In contrast, the T2WF HI showed large fluctuations and issued an alert at minute 52, while the T2WF indicator without parameter optimization issued an alert at minute 55. At the same time, in order to verify that the data at the 52nd minute did have faults, we generated a spectrogram for that period, as shown in Figure7. According to the empirical formula for the fault characteristic frequency of rolling bearings [33], there is an inner ring fault characteristic theoretical frequency of the base frequency multiplied by the constant 0.6 and then multiplied by the number of balls, resulting in 120 Hz. It can be clearly seen from the spectrogram that there is a clear fault at about 118 Hz characteristic frequency, which verifies the effectiveness of the proposed method.

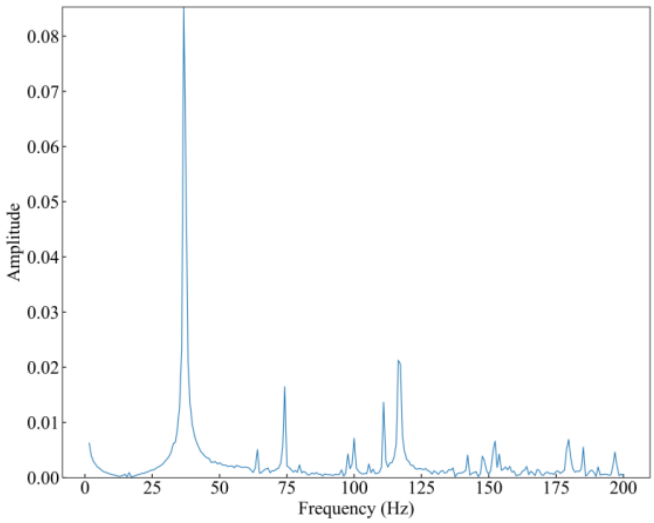

Figure 7. Frequency spectrum of bearing 2_2 at 52 minutes.

4.3. Comparison test of HI on petrochemical enterprise dataset

We conducted HI tests on the petrochemical enterprise dataset, and Figure 8 shows an example of time-domain signal processing for the collected dataset, (a) showing the vibration signal collected at the high-speed shaft measurement point, and (b) showing the vibration signal collected at the measurement point at the non-connected end of the high-pressure cylinder of the compressor. In this section of the experiment, the two monitoring methods commonly used in the industry are also

used for comparison and detailed results are presented. firstly, the upper limit of the 3σ confidence interval is calculated to be set as the warning threshold, which is compared with the historical HI data. the ISO standard [6] sets the warning threshold parameter for RMS at different power levels, and therefore the RMS warning threshold is set to be 5.5 mm/s. from the time the RMS The period from the beginning of the RMS curve to the 5.5 mm/s warning threshold is defined as the early failure stage.

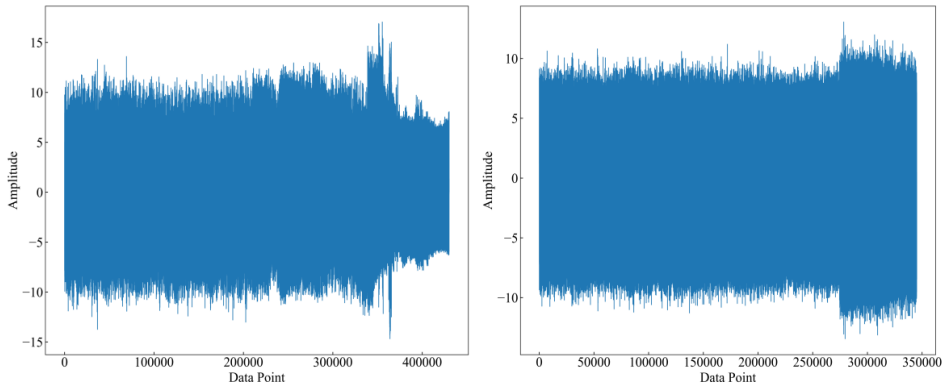

Figure 8. Time-domain visualization of the petrochemical enterprise dataset.

Figure 9 presents the time-domain variation of the proposed metrics for the main fan unit and the compressor equipment, as well as the spectrograms corresponding to the alarm moments. The upper part shows the time-domain variation, while the lower part illustrates the spectrograms at the corresponding alarm moments. It can be observed that in the early stage of the data, both sets of curves show relatively obvious fluctuation trends, especially in the file number of smaller intervals, the amplitude of the rise and close to the set threshold, indicating that the indicator in the early stage of the system state changes can produce a response. Compared with the traditional method, which tends to show anomalies at a later stage, this indicator has a strong dynamic sensitivity in the early stage. Specifically, the main fan unit shows a continuous increase in amplitude near the 100th file, while the compressor shows high frequency disturbances with increasing amplitude in the early and middle stages. This phenomenon suggests that the proposed indicator can reflect the potential anomaly evolution process in time and has potential application in early warning tasks.

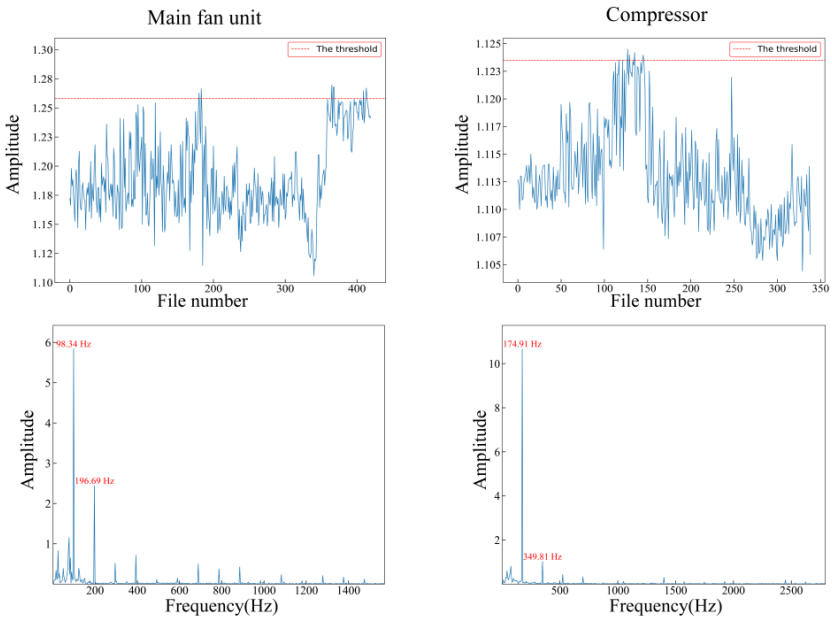

Figure 9. T2WF curve and corresponding frequency spectrum at the alarm time for the petrochemical enterprise dataset.

It should be introduced that when rotor misalignment occurs, its rotational frequency, and its octave frequency will appear significant high amplitude phenomenon, especially the second octave frequency will reach one-half of the rotational frequency, through the main fan's spectrogram in the figure it is not difficult to find that there is a clear component of the octave, and at the same time, the second octave frequency also reaches about one-half of the rotational frequency, which demonstrates a very typical feature. Fouling phenomenon occurs, the internal friction increases, resulting in an increase in the octave frequency of the rotational frequency, significantly higher than the other frequencies, in the compressor's spectrum diagram, the rotational frequency is accompanied by a clearer doubling frequency, doubling frequency, triple frequency, etc., thus confirming that the compressor's rotor is experiencing the phenomenon of fouling.

Table 7 First Alarm File for Each Indicator in Petrochemical Dataset a.

Indicator	Alert	Indicator	Alert
RMS	206	WF	377
SK	332	AE	351
PF	361	T2WF-NGOA	181
MEAN	321	T2WF	192

Table 8 First Alarm File for Each Indicator in Petrochemical Dataset b.

Indicator	Alert	Indicator	Alert
RMS	275	WF	246
SK	269	AE	157
PF	168	T2WF-NGOA	128
MEAN	178	T2WF	153

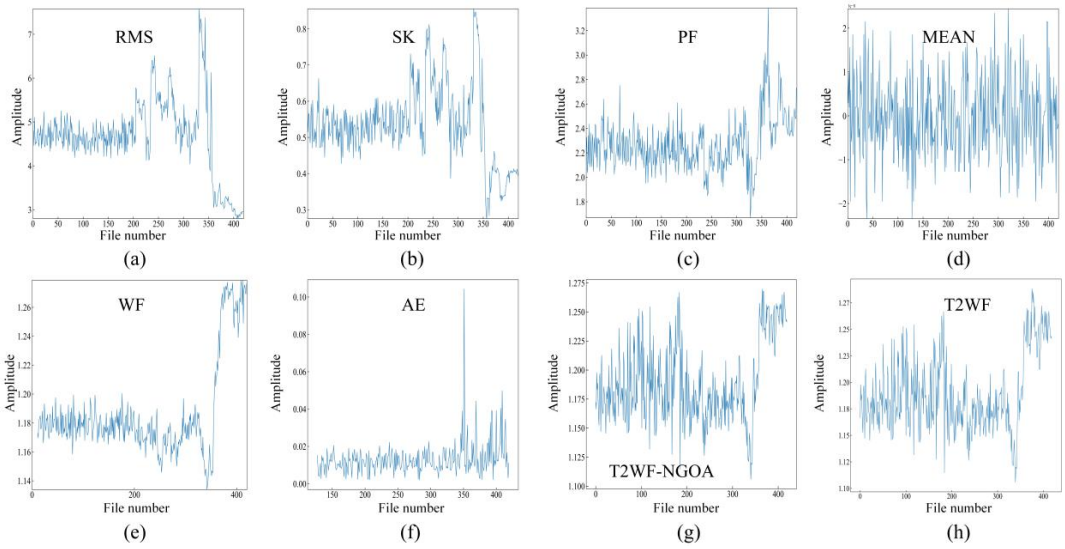

Figure 10. Monitoring curves for each indicator of petrochemical dataset a

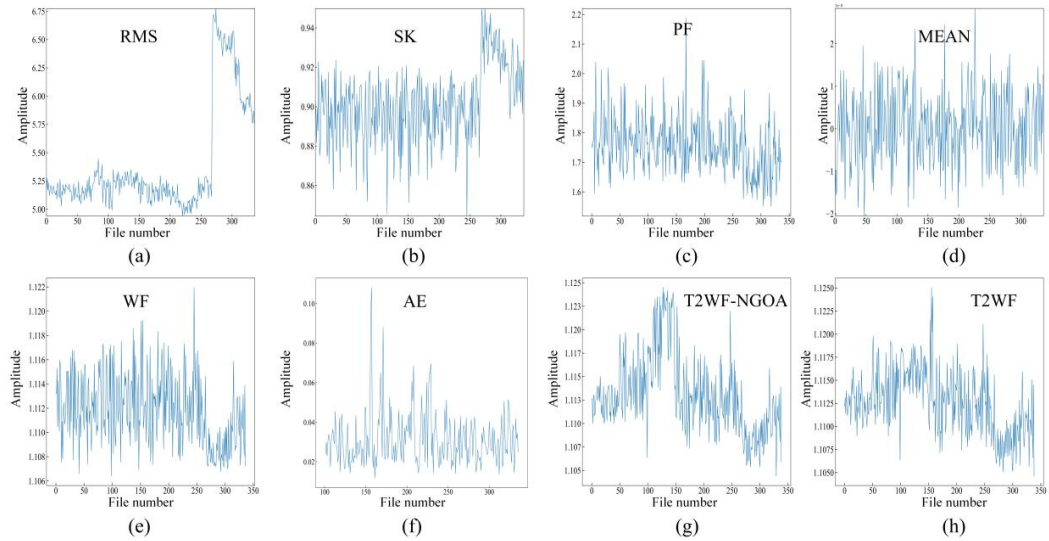

Figure 11. Monitoring curves for each indicator of petrochemical dataset b.

We show images comparing the results with other health metrics as well as with the AE method, the results for dataset a are shown in Table 7 and Figure 10, and the results for dataset b are shown in Table 8 and Figure 11. We perform a case-by-case analysis, for dataset a. The first time T2WF-NGOA crosses the warning threshold the number of files is 181 compared to 192 for the unoptimized T2WF, and the international standard specifies that the method has to be around 200 files at the earliest to trigger the warning. The international standard method requires the earliest alert to be around 200 file numbers, and the rest of the dimensionless metrics are between 321-377 before triggering the alert. This means that T2WF-NGOA shifts the warning point forward by about 9-10 % for the international standard, and by more than 50 % for traditional indicators such as WF. In the dataset b results, in the dynamic unbalance scenario caused by compressor rotor fouling, the first alarm number of T2WF-NGOA is only 128, while T2WF is 153, and the international standard method needs to wait until 275 files, and the rest of the traditional indicators are even later. Compared to the international standard, T2WF-NGOA shifts the alarm point forward by about 52 %; it maintains the earliest warning even when compared to complex methods such as AE reconstruction error. Figure 11 further shows that T2WF-NGOA crosses the threshold quickly from 110-130 and stays above the threshold for a long time in the following section, while the RMS and SK curves slowly accumulate to 150 before they are gradually triggered, and the WF and PF show high-frequency jittering only after 240.

In summary, the proposed T2WF-NGOA realizes the earliest and most robust early warning in both types of industrial scenarios, and the relevant comparison results provide clear support in both time and value levels, fully demonstrating its excellent robustness and foresight. From the perspective of mechanism, T2WF takes into account both short-term shocks and long-term trends by weighting proximal and distal periods, and adjusts their relative contributions through the weight, which enhances the early sensitivity of the model and its ability to adapt to different working conditions. Combined with the health index constructed by NGOA, T2WF-NGOA shows consistent early warning advantages on all types of datasets, highlighting its practical application potential in complex industrial scenarios.

5. Summary

In this paper, an innovative HI, T2WF is proposed with the aim of improving the sensitivity and accuracy of early failure monitoring of rotating machinery. The method effectively captures short-term abrupt changes and long-term trend information by fusing WF features in both proximal and distal periods and introducing an adjustable weighting mechanism. In order to further improve the performance of the index, the study introduces the NGOA to automate the tuning of the key parameters, so as to achieve the optimal fault characterization capability.

The experimental part is validated on the XJTU-SY public bearing dataset and the actual industrial data of two petrochemical companies respectively. The results show that the T2WF metric achieves earlier warning response than traditional health metrics (e.g., RMS, SK, WF, etc.) and some deep learning methods in several scenarios, demonstrating excellent advance and robustness. In petrochemical conditions, the metric even achieves more than 50% early warning lead time and is supported by clear fault characteristics at the spectral level.

In addition, the sensitivity of the key parameters of T2WF is also deeply analyzed in this paper, and it is found that the proximal period and weight M have a significant impact on the warning time, while the distal period is relatively stable, which provides a theoretical basis for the subsequent industrial deployment. The optimal parameters obtained from the global search of the parameter space via NGOA not only perform well on training data, but also migrate well in test and industrial data, further demonstrating the generalization capability of the proposed method.

In conclusion, T2WF-NGOA combines the time-weighting mechanism and intelligent optimization strategy to provide an efficient, robust and easy-to-deploy HI method for the early fault diagnosis of rotating machinery, which has strong potential for practical application under complex working conditions.

Bibliography

1. Zhou J, Yang J, Xiang S, Qin Y. Remaining useful life prediction methodologies with health indicator dependence for rotating machinery: A comprehensive review. IEEE Transactions on Instrumentation and Measurement 2025; 74: 1–19.

https://doi.org/10.1109/TIM.2025.3556919.
2. Jiang W, Wu J, Yang Y, Li X, Zhu H. Health evaluation techniques towards rotating machinery: A systematic literature review and implementation guideline. Reliability Engineering & System Safety 2025; 260: 110924. https://doi.org/10.1016/j.ress.2025.110924.
3. Zhou J, Yang J, Qin Y. A systematic overview of health indicator construction methods for rotating machinery. Engineering Applications of Artificial Intelligence 2024; 138: 109356. https://doi.org/10.1016/j.engappai.2024.109356.
4. Zhou H, Huang X, Wen G, Lei Z, Dong S, Zhang P, Chen X. Construction of health indicators for condition monitoring of rotating machinery: A review of the research. Expert Systems with Applications 2022; 203: 117297. https://doi.org/10.1016/j.eswa.2022.117297.
5. Bublil T, Cohen R, Kenett RS, Bortman J. Machine health indicators and digital twins. Sensors 2025; 25(7): 2246. https://doi.org/10.3390/s25072246.
6. ISO B and STANDARD B. Mechanical vibration—evaluation ofmachine vibration by measurements on non-rotating parts. Evaluation of machine vibration by measurements on non-rotating parts 2009.
7. Chu T, Nguyen T, Yoo H, Wang J. A review of vibration analysis and its applications. Heliyon 2024; 10(5): e26282. https://doi.org/10.1016/j.heliyon.2024.e26282.
8. Xin Y, Zhu J, Cai M, Zhao P, Zuo Q. Machine learning based mechanical fault diagnosis and detection methods: a systematic review. Measurement Science and Technology 2025; 36(1): 012004. https://doi.org/10.1088/1361-6501/ad8cf6.
9. Raj KK, Kumar S, Kumar RR. Systematic review of bearing component failure: Strategies for diagnosis and prognosis in rotating machinery. Arabian Journal for Science and Engineering 2025; 50: 5353–5375. https://doi.org/10.1007/s13369-024-09866-x.
10. Peng H, Zhao D, Shangguan L, Li S, Cheng R. Review of wind power bearing wear analysis and intelligent lubrication method research. Coatings 2024; 14(1): 30. https://doi.org/10.3390/coatings14010030.
11. Kundu P. Review of rotating machinery elements condition monitoring using acoustic emission signal. Expert Systems with Applications 2024; 252: 124169. https://doi.org/10.1016/j.eswa.2024.124169.
12. Chauhan S, Vashishtha G, Zimroz R. Analysing recent breakthroughs in fault diagnosis through sensor: A comprehensive overview. Computer Modeling in Engineering & Sciences 2024; 141(3): 1983. https://doi.org/10.32604/cmes.2024.055633.
13. Ni Q, Ji JC, Feng K. Data-driven prognostic scheme for bearings based on a novel health indicator and gated recurrent unit network. IEEE Transactions on Industrial Informatics 2023; 19(2): 1301–1311. https://doi.org/10.1109/TII.2022.3169465.
14. Song H, Sun Y, Gao H, Guo L, Wu T. A novel HI construction method based on healthy-state data training for rotating machinery components. Structural Health Monitoring 2024. https://doi.org/10.1177/14759217241279784.
15. Wang D, Zhong J, Li C, Peng Z. Box-Cox sparse measures: A new family of sparse measures constructed from kurtosis and negative entropy. Mechanical Systems and Signal Processing 2021; 160: 107930. https://doi.org/10.1016/j.ymssp.2021.107930.
16. Song S, Wang W. Early fault detection of rolling bearings based on time-varying filtering empirical mode decomposition and adaptive multipoint optimal minimum entropy deconvolution adjusted. Entropy 2023; 25(10): 1452. https://doi.org/10.3390/e25101452.
17. Hu Q, Si X, Zhang Q, Qin A. A rotating machinery fault diagnosis method based on multi-scale dimensionless indicators and random forests. Mechanical Systems and Signal Processing 2020; 139: 106609. https://doi.org/10.1016/j.ymssp.2019.106609.
18. Gao C, Lv K, Wu T, Si J, Hu Y. Method for determining starting point of rolling bearing life prediction based on linear regression. Electronics 2019; 8(9): 923. https://doi.org/10.3390/electronics8090923.
19. Neupane D, Bouadjenek M R, Dazeley R, Aryal S. Data-driven machinery fault diagnosis: A comprehensive review. Neurocomputing 2025; 627: 129588. https://doi.org/10.1016/j.neucom.2025.129588.
20. Yadav O P, Pahuja G L. Bearing health assessment using time domain analysis of vibration signal. International Journal of Image, Graphics and Signal Processing 2020; 11(3): 27. https://doi.org/10.5815/ijigsp.2020.03.04.
21. Miao Y, Zhao M, Hua J. Research on sparsity indexes for fault diagnosis of rotating machinery. Measurement 2020; 158: 107733. https://doi.org/10.1016/j.measurement.2020.107733.
22. Hidle E L, Hestmo R H, Adsen O S, Lange H, Vinogradov A. Early detection of subsurface fatigue cracks in rolling element bearings by the knowledge-based analysis of acoustic emission. Sensors 2022; 22(14): 5187. https://doi.org/10.3390/s22145187.
23. Hou B, Wang D, Xia T, Wang Y, Zhao Y, Tsui K-L. Investigations on quasi-arithmetic means for machine condition monitoring. Mechanical Systems and Signal Processing 2021; 151: 107451. https://doi.org/10.1016/j.ymssp.2020.107451.

24. Brusa E, Bruzzone F, Delprete C, Di Maggio L G, Rosso C. Health indicators construction for damage level assessment in bearing diagnostics: A proposal of an energetic approach based on envelope analysis. Applied Sciences 2020; 10(22): 8131. https://doi.org/10.3390/app10228131.
25. Zhang Q, Su N, Qin B, Sun G, Jing X, Hu S, Cai Y, Zhou L. Fault diagnosis for rotating machinery based on dimensionless indices: Current status, development, technologies, and future directions. Electronics 2024; 13(24): 4931. https://doi.org/10.3390/electronics13244931.
26. Vashishtha G, Chauhan S, Zimroz R, Kumar R, Gupta M K. Optimization of spectral kurtosis-based filtering through flow direction algorithm for early fault detection. Measurement 2025; 241: 115737. https://doi.org/10.1016/j.measurement.2024.115737.
27. Antoni J, Kestel K, Peeters C, Leclère Q, Girardin F, Ooijevaar T, Helsen J. On the design of optimal health indicators for early fault detection and their statistical thresholds. Mechanical Systems and Signal Processing 2024; 218: 111518. https://doi.org/10.1016/j.ymssp.2024.111518.
28. Dehghani M, Hubálovský Š, Trojovský P. Northern Goshawk Optimization: A new swarm-based algorithm for solving optimization problems. IEEE Access 2021; 9: 162059–162080. https://doi.org/10.1109/ACCESS.2021.3133286.
29. Adikaram K K L B, Hussein M A, Effenberger M, Becker T. Data transformation technique to improve the outlier detection power of Grubbs' test for data expected to follow linear relation. Journal of Applied Mathematics 2015; https://doi.org/10.1155/2015/708948.
30. Zhang C, Dong J, Zhang H, Liu X, Peng K. A novel process monitoring framework combined temporal feedback autoencoder and multilevel correlation analysis for large-scale industrial processes. Measurement 2024; 233: 114749. https://doi.org/10.1016/j.measurement.2024.114749.
31. Harrou F, Dairi A, Taghezouit B, Khaldi B, Sun Y. Automatic fault detection in grid-connected photovoltaic systems via variational autoencoder-based monitoring. Energy Conversion and Management 2024; 314: 118665. https://doi.org/10.1016/j.enconman.2024.118665.
32. Kibrete F, Woldemichael D E, Gebremedhen H S. Multi-sensor data fusion in intelligent fault diagnosis of rotating machines: A comprehensive review. Measurement 2024; 232: 114658. https://doi.org/10.1016/j.measurement.2024.114658.
33. Randall R B, Antoni J, Chobsaard S. The relationship between spectral correlation and envelope analysis in the diagnostics of bearing faults and other cyclostationary machine signals. Mechanical Systems and Signal Processing 2001; 15(5): 945–962. https://doi.org/10.1006/mssp.2001.1415.